TSUNAMI EVACUATION ROUTE MAPPING IN THE TEGALKAMULYAN AREA, CILACAP REGENCY BASED ON THE POTENTIAL OF A SOUTH JAVA EARTHQUAKE

Aliffia Retno Maya Saputri[1] , Muhamad Mahfud Muqoddas[2], Zaroh Irayani[1*]

[1] Jurusan Fisika, Fakultas MIPA, Universitas Jenderal Soedirman, Jl Dr. Soeparno No. 61, Purwokerto, 53123

[2] BMKG Stasiun Geofisika Banjarnegara, Jl. Raya Banjarmangu Km 12, Banjarnegara, 53452

*E-mail: zaroh.irayani@unsoed.ac.id

ABSTRACT

Cilacap Regency is one of the regions in Indonesia that is developing rapidly, especially in the oil mining industry. In terms of disaster vulnerability, the Cilacap Regency area has a high potential for a tsunami disaster because the region is located on the South Java subduction zone, so that if a large tsunami hits the Cilacap area and its surroundings, it will have a severe impact on coastal regions, one of which is the Tegalkamulyan area. As part of disaster mitigation efforts, tsunami evacuation route mapping was carried out using tsunami wave-propagation modeling based on the Shallow Water Equations (SWE). Tsunami simulations used three hypothetical earthquake sources in South Java, released by the National Earthquake Study Center in 2017, with magnitudes ranging from Mw 8.7. Scenario 5 is considered the worst-case scenario for tsunami modeling because it produces the most significant vertical displacement, with a wave increase of 11,418 m and a wave decrease of -7,476 m. Wave propagation shows that the tsunami waves propagated in all directions, with the fastest arrival time of 44 minutes and 1 second after the earthquake. The modeling results show a maximum inundation limit of 12,700 km from the coastline, with an area of 534,890 km2, and a maximum run-up height of 30,847 m. Based on the tsunami evacuation route map, vertical evacuation efforts directed people to immediately look for tall buildings and move towards Temporary Evacuation Sites with an estimated time of approximately 6 – 23 minutes on foot, while horizontal evacuation efforts directed people in Temporary Evacuation Sites to head to Final Evacuation Sites with an estimated time of approximately 13 – 20 minutes at an average speed of 38 km/h using motorized vehicles.

Keywords: tsunami modeling, Shallow Water Equations, inundation, mitigation, evacuation routes

1. Introduction

Cilacap Regency is one of the regions in Indonesia that is rapidly developing in terms of infrastructure. Most of the development centers in Cilacap Regency are located in coastal areas, especially in oil-mining regions [1]. The Cilacap Regency area is also a tourist destination, especially for beach tourism, thanks to its beautiful coastal views. In terms of disaster vulnerability, the Cilacap Regency area has a significant potential for tsunami disasters because it lies within the South Java subduction zone, where the Indo-Australian Plate subducts beneath the Eurasian Plate. Cilacap Regency is the most tsunami-prone district in Central Java Province and the third-most tsunami-prone in Indonesia [2], so if a large tsunami hits the Cilacap area and its surroundings, it will have a severe impact on coastal areas with a reasonably high population density.

A tsunami occurred at Pangandaran Beach on July 17, 2006, originating from an earthquake of Mw 7.7. The tsunami with a water height reaching 4 meters impacted the Cilacap tourist area, damaging 64 houses and causing 105 casualties, including 98 people died and seven others were injured. The tsunami caused by this earthquake resulted from the thrust of a tectonic fault centered at 9.22° S and 107.32° E, at a depth of 34 km [3]. Research by Widiyantoro et al. showed that in the developed scenario, there is a high potential for a megathrust event off the coast of South Java, as indicated by the seismic gap along the Java Trench [4]. This is reinforced by a statement from Heri Andreas, as Chair of the Disaster Research Institute of the Bandung Institute of Technology Alumni Association (IA-ITB), who stated that one of the sources of the earthquake was the South Java Megathrust. Earthquakes cannot be accurately predicted to date, despite extensive research into earthquake precursors [5].

South Cilacap District is one of six districts potentially affected by a tsunami. A closer look at the tsunami hazard map published by the BMKG Banjarnegara Geophysical Station [6] shows that the Tegalkamulyan area is the most vulnerable to tsunami threats. This Area is located on the coast of South Cilacap District, which has a relatively highpopulation density. There is a lot of human

Tsunami Evacuating Route Mapping..Aliffia Retno Maya Saputri, et. al

133

activity in the Area, thus increasing the risk of a tsunami.

Tsunami modeling generally uses computer-assisted numerical methods to speed up the evaluation of mathematical formulas that simulate the transformation of coastal physical objects. COMCOT (Cornell Multi-grid Coupled Tsunami model) is a software that functions to generate tsunami propagation from the epicenter using the Shallow Water Equations (SWE) approach, consisting of mass conservation equations and momentum conservation equations. To balance efficiency and accuracy, the grid system is determined using the leapfrog finite-difference method, with linear or nonlinear parts adjusted for each layer. Larger grid sizes can be used in the open sea to study tsunami propagation, and finer grids can be adopted for coastal areas of interest [7]. Through this tsunami modeling, an overview of the design of the tsunami source, tsunami wave propagation, tsunami wave arrival time, tsunami wave overflow, and the Area affected by the tsunami can be obtained. This can serve as a basis for creating hazard and evacuation route maps as a reference for developing preparedness and evacuation strategies in tsunami disaster mitigation efforts in the study area.

Earthquake. Tectonic earthquakes are the dominant cause of tsunamis in Indonesia. Earthquakes capable of generating tsunamis are commonly referred to as tsunamigenic earthquakes. These earthquakes must have significant seismic moments and shallow epicenters to cause seafloor deformation. The relationship between seismic moment and dislocation of the seafloor fault plane can be seen in the following equation [8]:

$$Mo = \mu \, d \, A \qquad (1)$$

Where Mo is the seismic moment (Nm), μ represents rigidity (N/m^2), d represents deformation or dislocation (m), and A represents the area of the fault plane (m^2).

Earthquake magnitude is not suitable for small-scale earthquakes because slip displacement is relatively small or even negligible [9]. The relationship between earthquake magnitude and seismic moment can be seen in the following equation [10]:

$$M_w = \frac{2}{3} \left[\log M_o - 10{,}7 \right] \qquad (2)$$

Earthquake parameters related to tsunami formation include seismic moment, epicenter location, hypocenter, focal mechanism, and fault geometry. The scaling law method is used to determine the main fault-zone parameters' length and width, while strike, dip, and slip are obtained from regional geological data and previous studies. These parameters are used to create numerical model designs and initial conditions for tsunami wave propagation. The moment magnitude (Mw) determines the size of the fault (length, width), which can be determined based on the distribution of earthquake occurrences by interpolating based on the following equation [11]:

Fault Length (L):

$$Log \, L = 0{,}58 \, M_w - 2{,}42 \qquad (3)$$

Fault Width (W):

$$Log \, W = 0{,}41 \, M_w - 1{,}61 \qquad (4)$$

Tsunami. Tsunamis are long-period ocean waves caused by impulsive disturbances in the ocean floor due to tectonic activity, volcanic eruptions, or underwater landslides [12]. Impulsive disturbances cause deformation of the seabed, which displaces the volume of water above it. Vertical deformation of the ocean floor due to fault shifts can raise or lower sea levels on a large scale. Sea levels will rise suddenly when the ocean floor increases due to a thrust fault, as illustrated in the following figure.
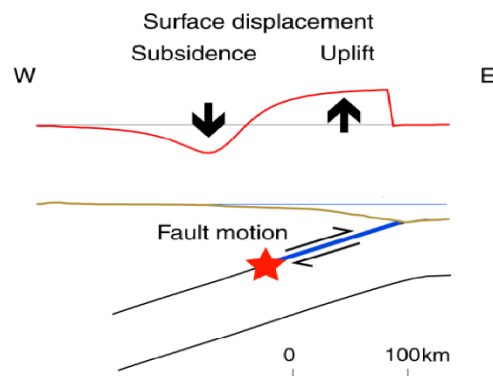

Figure 1. Movement of the seabed tsunami source following the deformation of the fault plane [13].

The speed of a tsunami wave can accelerate or slow down depending on the ocean depth. As the ocean depth decreases, the tsunami speed decreases. This phenomenon can be explained by the following equation [7]:

$$v = \sqrt{g \, h} \quad \text{dan} \quad \lambda = v \, T \qquad (5)$$

Where v is the tsunami wave speed (m/s), g is the gravitational acceleration (m/s^2), which is 9.8 m/s^2, h is the bathymetric depth (m), λ is the tsunami wavelength (m), and T is the wave period (s).

When tsunami waves enter coastal waters, their motion slows, and their wavelengths shorten. This phenomenon occurs because tsunami waves slow down as they enter shallow water. The wave energy is focused vertically, increasing wave height (shoaling effect), while the tsunami period remains relatively constant. As a result, the waves can break, causing extensive damage. Figure 2 shows the relationship between tsunami speed, wavelength, and ocean depth. Tsunami waves entering shallow water

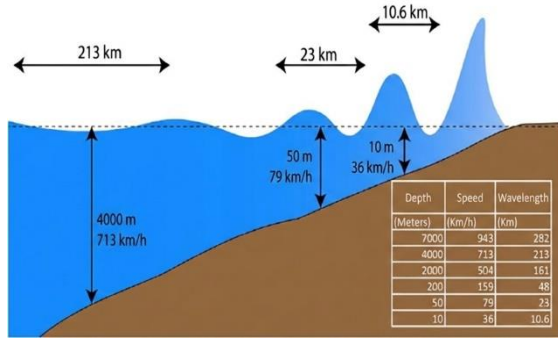will undergo wave transformation, as shown in Figure 3.

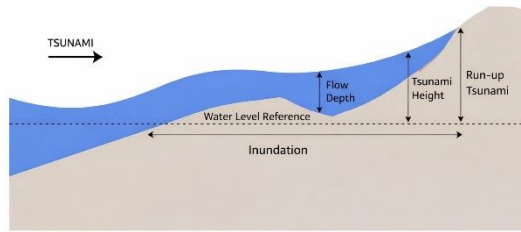Figure 2. Relationship between tsunami speed and wavelength and sea depth [14].

Figure 3. Illustration of tsunami parameters [15].

Tsunami Wave Propagation Equation. Tsunamis are classified as long waves because the water depth is much smaller than the wavelength of the tsunami. Under these conditions, the vertical acceleration of water particles can be ignored, and the horizontal velocity of water particles is considered uniform from the bottom to the surface of the water. Based on this approach, long waves are well suited to shallow-water theory [16].

The shallow-water theory explains that the propagation of long waves, such as tsunamis, is influenced by ocean depth. This theory, both in linear and nonlinear forms, is implemented in the COMCOT software using Cartesian and spherical coordinates. As tsunami waves enter the continental shelf and approach the coast, the wavelength of the incoming tsunami becomes shorter, and its amplitude becomes larger because the main tsunami wave propagates into shallow water. Therefore, the nonlinear convective inertia force and the bottom friction term become increasingly important, while the Coriolis force and the frequency dispersion term decrease [17].

Wang explains that along the coastline where the water depth is zero, special treatment is required to track the coastline's movement [18]. When the simulation involves a relatively small area where the rotation of the earth does not affect, it is more often used in Cartesian coordinates. The equations used in tsunami modeling are the nonlinear Shallow Water Equations (SWE) equations, which consist of the mass conservation equations in equation (6) and the momentum conservation equations in equations (7) and (8).

Conservation of mass equation:

$$\frac{\partial \eta}{\partial t} + \left(\frac{\partial M}{\partial x} + \frac{\partial N}{\partial y} \right) = 0 \tag{6}$$

Conservation of momentum equation:

$$\frac{\partial M}{\partial t} + \frac{\partial}{\partial x}\left(\frac{M^2}{D} \right) + \frac{\partial}{\partial y}\left(\frac{MN}{D} \right) + gD\frac{\partial \eta}{\partial x} + F_x = 0 \tag{7}$$

$$\frac{\partial N}{\partial t} + \frac{\partial}{\partial y}\left(\frac{N^2}{D} \right) + \frac{\partial}{\partial x}\left(\frac{MN}{D} \right) + gD\frac{\partial \eta}{\partial y} + F_y = 0 \tag{8}$$

Where η is the sea level elevation (m), t shows time (s), M is the x-direction flux (m²/s), N is the y-direction flux (m²/s), with $D = \eta + h$ shows the total depth of sea water (m), h is the bathymetric depth (m), and g is the acceleration due to gravity (m/s²) of 9.8 m/s². At the same time, Fx and Fy denote the bottom friction in the X and Y directions, respectively. These two terms are evaluated through the Manning formula, where n is the Manning roughness coefficient [18]:

$$F_x = \frac{gn^2}{D^{\frac{7}{3}}} M\sqrt{M^2 + N^2} = 0 \tag{9}$$

$$F_y = \frac{gn^2}{D^{\frac{7}{3}}} N\sqrt{M^2 + N^2} = 0 \tag{10}$$

If the value of the friction term approaches zero, then the nonlinear effect can be ignored, so that equations (7) and (8) can be solved linearly with the following equations [16]:

$$\frac{\partial M}{\partial t} + gD\frac{\partial \eta}{\partial x} = 0 \tag{11}$$

$$\frac{\partial N}{\partial t} + gD\frac{\partial \eta}{\partial y} = 0 \tag{12}$$

Tsunami Disaster Mitigation. Natural disasters are unpredictable, but in theory, tsunamis are easier to predict than earthquakes. In the far-field region, there is a delay of approximately 20–30 minutes before the tsunami wave reaches the coast. However, for near-field tsunamis, the arrival time can be much shorter (less than 10 minutes), so early warning systems must account for this. An analysis of the earthquake's characteristics can determine whether it is capable of causing a tsunami. This information can be immediately communicated to the public before a tsunami wave hits the coast [19]. Vigilance is part of disaster mitigation and can be achieved through preparedness, taking steps early to minimize damage and avoid loss of life in areas with potential tsunami impact [20].

Emergency response planning, including the availability of evacuation locations, evacuation times, evacuation routes, and alternative actions, is essential for preparedness. The general policy for implementing the tsunami disaster risk reduction master plan aims to protect the community from the threat of tsunamis by providing Temporary Evacuation Sites (TES)/Shelters, which must be supported by evacuation routes as determined by the mapping results. It is necessary to prepare evacuation routes and stairs, including evacuation road/access plans, from tsunami-prone areas to safe places [21].

2. Methods

Based on data from PuSGeN in 2017 [22], it is predicted that earthquakes in South Java could reach a magnitude of Mw 8.7. In addition, the bathymetric data were from GEBCO in 2021 [23], the topographic data were from DEMNAS in 2018 [24], and the Manning roughness value was taken from Muqoddas's research, which was adjusted for conditions on the Cilacap coast [25]. Tsunami modeling is generally based on data on the earthquake source mechanism. To determine the parameters of the tsunami-generating earthquake, the scaling law is

used to obtain fault lengths of 420 km and 90 km. Based on the fault length, the model does not match the geological conditions of the fault area, so the model is divided into three segments to ensure the fault's strike matches that of the South Java subduction. To determine the impact of using the Manning roughness classification on land to the maximum, the modeling is made with an earthquake source perpendicular to the research area of the Java Trench. The fault geometry is at least 30 km from the trench, so it is excluded from the sediment section. The strike, dip, and depth angle values are obtained from USGS slab 1.0 data, and the slip value is given 90° to maximize tsunami inundation. Using the depth value, a rock rigidity value (μ) of 3×10^{10} Pa was obtained, which refers to the classification results [26]. This value was used because the southern Java subduction zone has rock characteristics comparable to those of other Indo-Australian subduction zones, making it relevant for earthquake source simulations. The complete parameters of the earthquake source that generated the tsunami are shown in Table 1, and the determination of the earthquake source model is shown in Figure 4.

Table 1. Hypothetical earthquake model of tsunami generation.

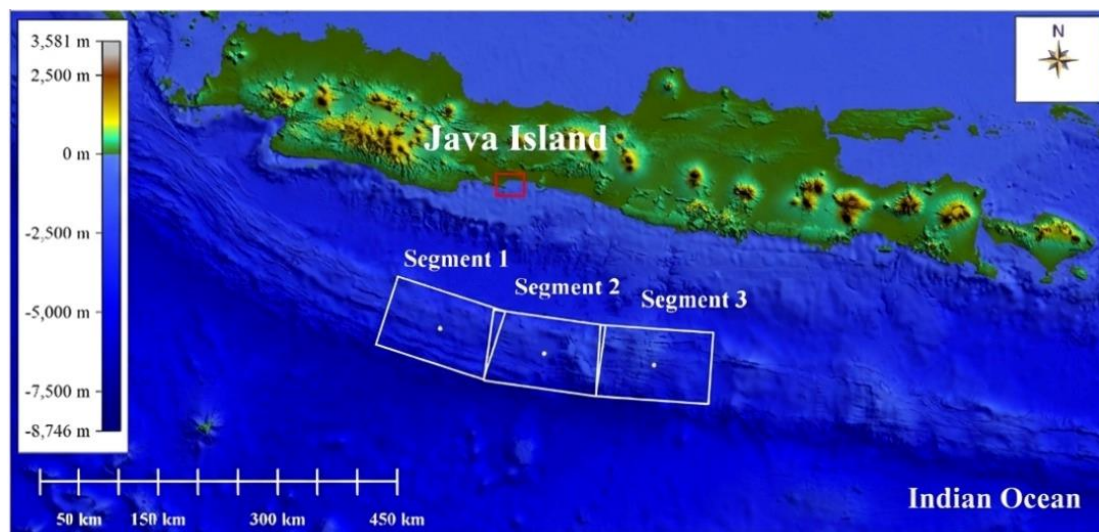| Earthquake Source	Epicenter		Dimensions (km)		Source Mechanism (°)			Depth (km)	Rigidity (Pa)	Disloc (m)	Mo	Mw
	Long	Lat	L	W	θ	d	λ					
Segment 1	108.30	-9.35	140	90	288	9	90	18.5	20×10^9	26	6.55×10^{21}	8.5
Segment 2	109.47	-9.64	140	90	278	11	90	15.3	15×10^9	26	4.91×10^{21}	8.4
Segment 3	110.72	-9.77	140	90	273	13	90	15.7	16×10^9	26	5.24×10^{21}	8.4
Total (earthquakes occur simultaneously)											1.67×10^{22}	8.7

Figure 4. Earthquake segmentation model.

The modeling was conducted using five scenarios based on earthquakes originating from the three segments. The tsunami modeling scenarios are presented in Table 2. The first scenario is an earthquake originating from segment 1 with a magnitude of 8.5. The second scenario is an earthquake originating from segment 2 with a magnitude of 8.4. The third scenario is an earthquake originating from segment 3 with a magnitude of 8.4. The fourth scenario is an earthquake originating from all three segments co-occurring with a magnitude of 8.7. The fifth scenario is an earthquake originating from all three segments with different rupture durations. Based on the research of Khoiridah and Santosa, who calculated the rupture duration in modeling the vertical deformation of earthquake sources as a study of the potential tsunami hazard in the South Java Sea, it shows that earthquakes with a magnitude of >5.5 SR have a rupture duration (Tdur) of ≤78.04 s [27]. In this study, a Tdur of 75 s was used: the first earthquake at 0 s, the second at 25 s, and the third at 50 s.

Table 2. Tsunami modeling scenario and earthquake time.

Scenario	Earthquake Source Tsunami Generator		
	Segment1	*Segment2*	*Segment3*
1	0 s	-	-
2	-	0 s	-
3	-	-	0 s
4	0 s	0 s	0 s
5	50 s	25 s	0 s

Furthermore, the rupture propagation direction starts at the easternmost segment and proceeds to the westernmost segment. The rupture propagation direction is based on the 2004 tsunami-generating earthquake in Aceh, which indicated that plate subduction originated from the southeast. The earthquake strength for the fifth scenario is based on integrating seismic moments from all segments, yielding an earthquake with a magnitude of Mw 8.7.

Tsunami modeling uses the COMCOT software in Fortran. The output from COMCOT includes the initial tsunami condition, height, and time for each step. The initial tsunami source profile can be obtained from the initial tsunami condition as a vertical displacement, i.e., the seabed deformation. Tsunami wave propagation (snapshots) shows the movement of the water column at each time period after the earthquake. The tsunami wave overtopping can be observed from the modeled tsunami run-up height.

Creation of Tsunami Evacuation Routes. Tsunami disaster risk reduction efforts can be carried out by identifying tsunami evacuation routes and locations in tsunami-prone areas. Evacuation route planning aims to minimize the negative impacts of disasters and to find the shortest path to safe places for people living in disaster-prone areas. When estimating the arrival time of a tsunami wave, not all time can be used for evacuation; there is time to detect the tsunami, time to prepare, and time to climb to a safe position. Evacuation routes direct residents away from the direction of wave propagation and must be clearly indicated by signs, such as away from the coastline; avoid roads parallel to the coastline; avoid river basins; towards roads with wider widths to avoid bottlenecks (narrow paths); and the movement of masses in each block is directed so that they do not mix with other blocks to avoid traffic jams (traffic jams). Evacuation methods are divided into two: vertical and horizontal. The vertical evacuation method directs evacuees to safe areas within the tsunami's reach, in this case to Temporary Evacuation Sites (TES). The horizontal evacuation method directs refugees to a secure area beyond the tsunami's reach, in this case to the Final Evacuation Point (TEA) [28].
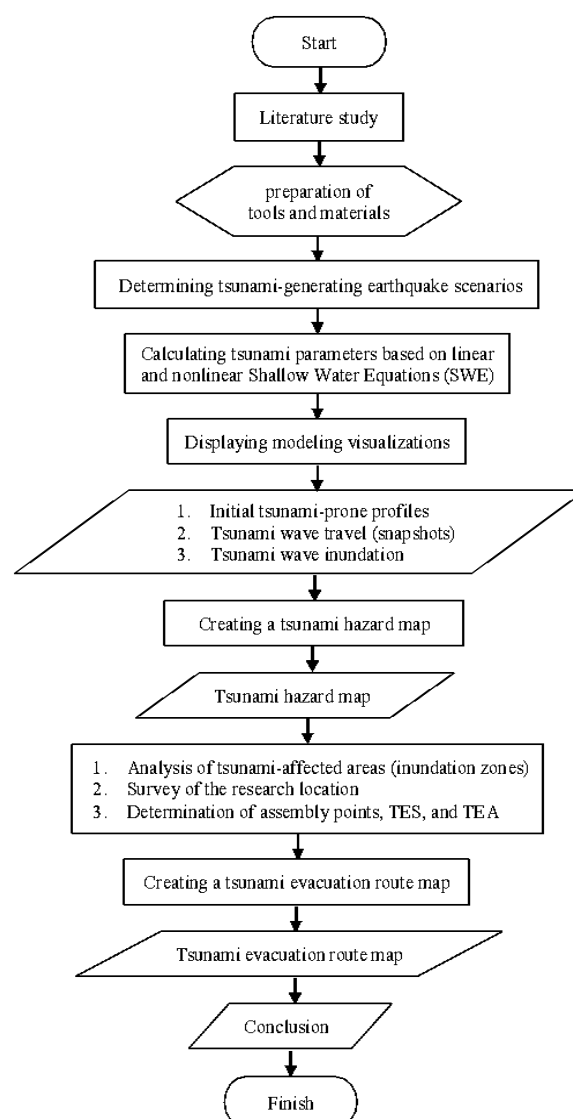

Figure 5. Research flowchart

Tsunami Evacuating Route Mapping...Aliffia Retno Maya Saputri, et. al

137

3. Results and Discussion

Tsunami Source Design. The initial conditions for a tsunami indicate the uplift and subsidence of the seabed, caused by sudden shifts in the Earth's layers that move the water column. Layer 1 was chosen as the modeling input because it encompasses the earthquake's epicenter and the study area.

Figure 6 shows the initial conditions of a tsunami, depicting changes in sea level around the epicenter. The deformed seabed will result in vertical displacement, with sea level rise indicated by the red sea area and sea level fall indicated by the dark blue sea area. The sea level fall value will be negative, indicating a wave height below Mean Sea Level (MSL). The epicenter location and the earthquake source strength strongly influence the initial conditions of a tsunami. Changes in sea level around the epicenter are presented in Table 3. Across all modeled scenarios, differences in the tsunami's initial conditions are visible. These differences are caused by differences in the strength of the earthquake source generating the tsunami, as shown in Table 1.
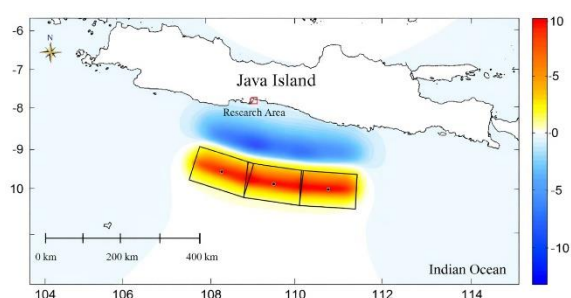

Figure 6. Initial tsunami conditions for the worst case scenario.

Table 3. Sea level changes in initial tsunami conditions.

Scenario	Sea Level Changes	
	Rise (m)	Decrease (m)
1	9,554	-5,399
2	10,203	-5,006
3	10,520	-4,530
4	11,868	-7,605
5	11,418	-7,476

The greater the earthquake's magnitude, the greater the deformation of the seafloor. Differences in fault geometry (strike, dip, and slip) also influence the deformation. These parameters will affect the magnitude of sea level rise and fall around the earthquake's epicenter.

Tsunami Wave Propagation. The tsunami modeling in this study was conducted over a 5-hour simulation period, with wave propagation models changing every 15 seconds. After the modeling, several snapshot patterns (tsunami wave propagation) were obtained for each time period after the earthquake.

The snapshot modeling was performed on layer 1, the largest layer, enabling visualization of how tsunami waves propagated from the earthquake epicenter to land.

The propagation of tsunami waves in layer one is shown in Figure 7, where the color scale from blue to red on the right side of the image indicates wave height. Modeling results suggest that tsunami waves propagate from the earthquake source in all directions. As tsunami waves approach the coast, their wavelength decreases, but their amplitude increases because the tsunami wave speed depends on water depth.
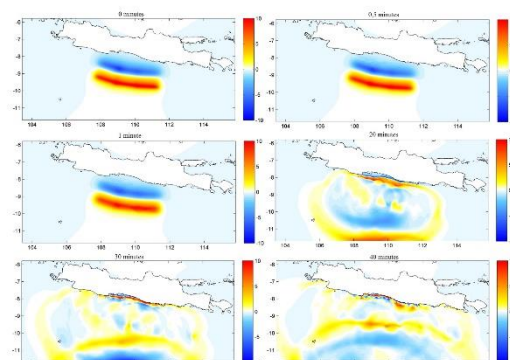

Figure 7. Layer 1 Snapshot for worst case scenario.

Snapshot modeling was also performed on layer 5, the smallest layer. This layer is the primary focus of the research, allowing for a clearer view of how tsunami waves propagate as they enter and impact the land. Figure 8 shows the propagation of tsunami waves in layer 5. The modeling results indicate that in the first minutes after the earthquake, the sea level recedes along the coastline. High waves begin to appear along the coastline 30 minutes after the quake, then move onto land and affect it for several kilometers. Based on wave height and the land area affected by the tsunami, the fifth scenario is the worst-case among all models.

Tsunamis experience energy distribution due to wave elongation during their journey from shallow to deep parts, and energy compression due to wave shortening. In addition to changes in shape due to their nonlinear Nature, changes in waves or tsunami transformations can occur due to changes in length and height (shoaling), changes in wave direction (refraction), wave propagation to protected areas (diffraction), and propagation due to reflection by nature or buildings (reflection) [29]. Rising waves are dangerous and can reach land, damaging human settlements. Meanwhile, receding tsunami waves are also dangerous because they can drag and carry material on the coast.
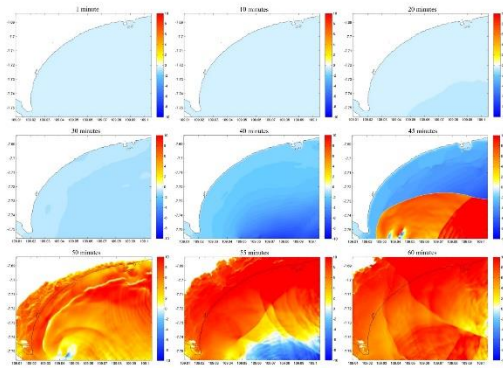
Figure 8. Layer 5 snapshot for worst case scenario.

Tsunami Wave Arrival Time. Virtual tide gauges are used to predict travel time and tsunami wave height. The observation points are plotted in Figure 6, which shows the positions of four virtual tide gauges relative to the earthquake source and the direction of tsunami wave propagation. The estimated tsunami arrival time is the time it takes for a wave to reach a coastal area, calculated after the tsunami-generating earthquake. Tsunami wave heights modeled at a virtual tide gauge can serve as warnings to residents. The Meteorology, Climatology, and Geophysics Agency (BMKG) issues tsunami threat estimates divided into four hazard categories based on maximum wave height: low (<1 m), moderate (1–3 m), high (3–6 m), and very high (>6 m). Based on tsunami wave propagation modeling results, the Tegalkamulyan area is classified as a threat area with a warning level. Figure 8 shows wave elevations based on a virtual tide gauge installed near the coast at a specific depth. Wave propagation is influenced by the bathymetric structure of the seabed from the earthquake epicenter to land. After the earthquake, the sea level receded, as evidenced by the negative wave height at each observation point (virtual tide gauge) in the initial minutes (below the MSL value). The tsunami wave arrival time is based on the status (warning level) from the BMKG. After the receding period, the wave will rise again, and when it reaches 0.5 m, it can be predicted to have reached land. The circle symbol in Figure 9 indicates the fastest time for the wave to arrive, and the star symbol indicates the maximum height of the tsunami wave that reaches land.

The greater the strength of the tsunami-generating earthquake, the greater the vertical deformation on the seabed, so the faster the arrival time and the higher the tsunami waves that hit, the more pronounced the resulting data are observed in Tables 4 and 5. The arrival time of the tsunami wave depends on its distance from the earthquake source; the closer it is, the faster it propagates. Wave propagation starts from virtual tide gauge one, which is located closest to the earthquake source location, to virtual tide gauge five, which is located furthest from the earthquake source location. Across all modeled scenarios, virtual tide gauge 1 has a shorter arrival time than the other virtual tide gauges farther from the earthquake source. The maximum height of the tsunami wave occurs almost entirely at virtual tide gauge 5, because it is close to the flow of the Serayu River. Areas near river flows are tsunami-prone areas. This Area has the potential to become a path for tsunami wave propagation [2].
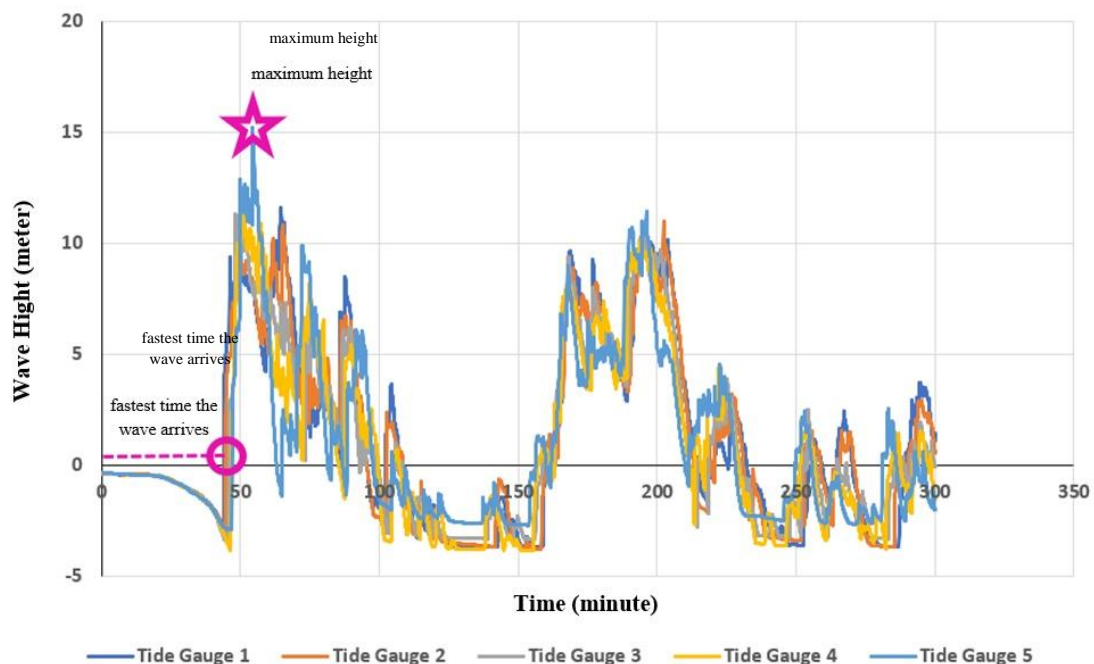

Figure 9. Wave propagation graph based on virtual tide gauge for worst case scenario.

Table 4. Tsunami wave arrival time.

Scenario	*Virtual Tide Gauge*	Coordinate *Virtual Tide Gauge*		Time to Arrive (hour:minute:second)
		Longitude	Latitude	
1	1	109,024	-7,736	00:44:34
2	1	109,024	-7,736	00:46:58
3	1	109,024	-7,736	00:58:21
4	1	109,024	-7,736	00:44:01
5	1	109,024	-7,736	00:44:34

Table 5. Maximum tsunami wave height and time.

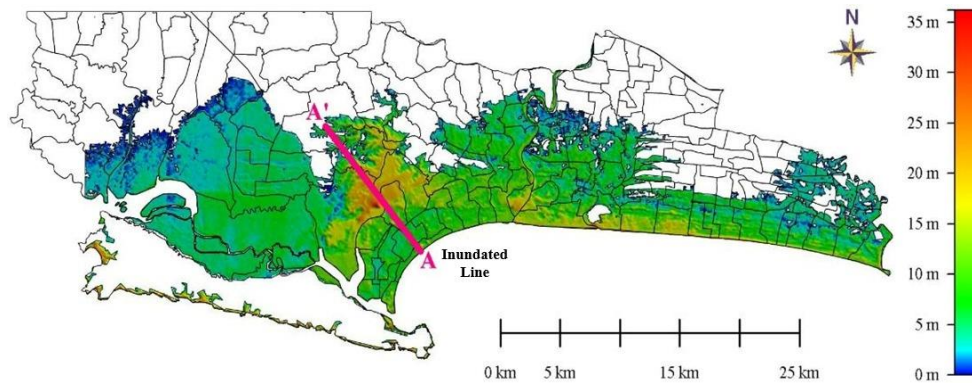| Scenario	*Virtual Tide Gauge*	Coordinate *Virtual Tide Gauge*		Maximum Height (meter)	Maximum Altitude Time (hour:minute:second)
		Longitude	Latitude		
1	5	109,073	-7,695	9,139	00:50:04
2	5	109,073	-7,695	9,016	00:58:02
3	1	109,024	-7,736	9,892	04:59:33
4	5	109,073	-7,695	15,214	00:54:22
5	5	109,073	-7,695	14,468	00:54:46

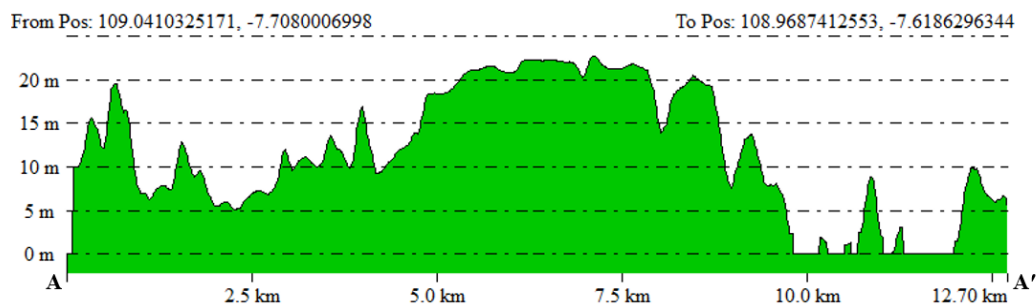Figure 10. Tsunami Wave Overflow for Worst Case Scenario.

Figure 11. Tsunami Wave Height at the Inundation Line for the Worst Case Scenario.

Tsunami Wave Overflow and Inundation Area.
The Area affected by a tsunami can be calculated based on the tsunami wave overflow model over land. The tsunami run-up height influences this model. Figure 10 shows the tsunami wave overflow model over land, and Figure 11 shows the tsunami wave height at the inundation line for the worst-case scenario (scenario 5). The tsunami wave overflows the land and has different heights in different regions. The inundation distance, or the farthest distance the tsunami hits land, is calculated horizontally and perpendicularly from the coastline. The inundation

distance in Figure 10 is calculated from A – A′, indicated by the pink line. Figure 11 shows the tsunami wave height at the inundation line, calculated vertically from the sea level. The tsunami run-up height is at point A′, measured vertically from the average sea level.

Modeling results indicate that tsunami waves propagated along the coast in Cilacap Regency. Differences in tsunami wave run-up over land affected the extent of the tsunami impact. The resulting data are shown in Table 6. The varying run-

up values are due to the earthquake's magnitude and the distance from the epicenter to each Area. In addition, several other factors influence the differences in run-up values, including bathymetry, coastal morphology, and tsunami wave height. This phenomenon is followed by a shoaling effect that increases the height of the tsunami waves. Coastal morphology primarily determines how far a tsunami can travel to land. On steep coasts, tsunami waves will not penetrate far inland because they are held back and reflected by the coastal cliffs. Meanwhile, on gently sloping coasts, tsunami waves will penetrate and hit inland for several kilometers.

Tsunami Hazard Map. The results of tsunami wave-propagation modeling show that the wave arrival time, run-up height, and inundation differ. Differences in earthquake magnitude cause these differences in values: the distance from the earthquake epicenter to each Area, bathymetric

profiles, coastal shape, coastal slope, and tsunami wave height. Based on the first, second, third, fourth, and fifth scenarios, the worst-case scenario can be modeled. Latief et al. conducted modeling and mapping of tsunami inundation and a tsunami disaster risk study in Padang City, explaining that tsunami danger can be determined by wave height. The classification of tsunami danger levels based on wave height is shown in Table 7 [30].

Figure 12 shows a tsunami hazard map for the Tegalkamulyan area for a worst-case scenario. Nearly all of Tegalkamulyan falls into the very high-risk category, with several regions also showing high risk. The maximum tsunami wave height reached 13,540 m, symbolized by the dark blue triangle. The minimum tsunami wave height reached 2,089 m, symbolized by the light blue triangle.

Table 6. Affected Area, Inundation Distance, and Run-Up Height.

Scenario	Affected Area (km²)	Inundation Distance(km)	Topographic height (m)	High Flow Depth (m)	Run-Up Height (m)
1	276,290	9,280	14,049	1,470	15,519
2	323,850	8,700	15,725	3,430	19,155
3	98,145	1,670	5,996	0.520	6,516
4	406,340	9,380	21,798	0.450	21,798
5	534,890	12,700	27,007	3,840	30,847

Table 7. Tsunami Hazard Level Classification Based on Wave Height.

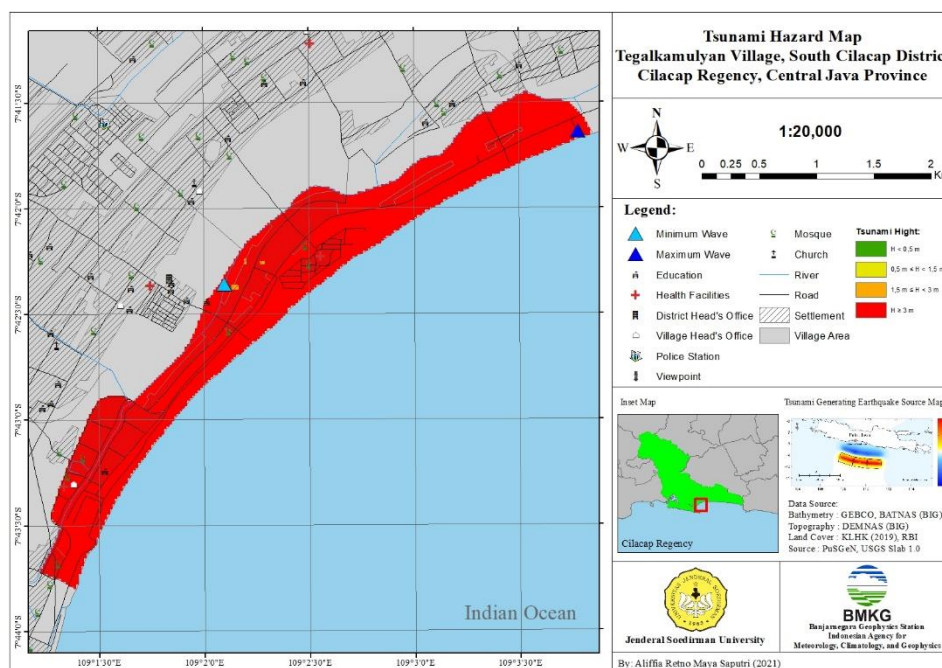| Tsunami Wave Height	Hazard Level Classification
H ≥ 3 m	Very Dangerous
1.5 m ≤ H < 3 m	Danger
0.5 m ≤ H < 1.5 m	Quite Dangerous
H < 0.5 m	No Danger

Figure 12. Tsunami Hazard Map of Tegalkamulyan Village for the Worst Case Scenario.

Tsunami Evacuation Route Map. The results of tsunami wave propagation modeling indicate that tsunami waves arrive at the coast of the Tegalkamulyan area 44-58 minutes after the earthquake. The fastest time for the waves to come for the worst-case scenario (scenario 5) is 44 minutes and 1 second after the quake. This underlies the need for a tsunami early warning system center. Cilacap City is already connected to INA TEWS (Indonesian Tsunami Early Warning System) and has a tsunami warning siren. Information calculated by the BMKG will be sent to the local government, specifically the Pusdalops (Operations Control Center) of the local BPBD, and disseminated to the public.

Figure 13 shows a tsunami evacuation route map for the Tegalkamulyan area, created from a worst-case tsunami hazard map. This map directs evacuees to evacuation sites. Tegalkamulyan Village is located in a coastal area with a high tsunami inundation risk. Vertical evacuation efforts directed residents to immediately seek high-rise buildings and move to Temporary Evacuation Sites (TES). To avoid crowding, the evacuation of the Tegalkamulyan community was divided into several Temporary Evacuation Sites (TES) as listed in Table 8, which met earthquake and tsunami resistance standards.

Horizontal evacuation efforts will direct residents at Temporary Evacuation Sites to the Final Evacuation Site (TEA). To avoid traffic jams, BPBD, TNI, and other relevant agencies coordinated vehicle traffic and evacuation efforts to keep the route to Tunggul Wulung Airport clear during the evacuation. Tunggul Wulung Airport is located 23 meters above sea level, far from the coast, preventing the tsunami from inundating the Area. It has a 1,400-meter-long, 30-meter-wide runway and a 777-square-meter terminal, making it large enough to accommodate a large number of evacuees. The estimated time to reach the airport is approximately 13–20 minutes at an average speed of 38 km/h by motorized vehicle.

Table 8. Temporary evacuation locations and estimated evacuation time for the Tegalkamulyan community.

| Tsunami-Prone Areas	Temporary Evacuation Site	Distance to Evacuation Site (km)	Estimated Evacuation Time by Foot (minutes)
South Karangmulia	Fave Hotel	± 0.8	6 – 8
North Karangmulia	Cilacap State Polytechnic	± 1.3	10 – 12
Central Karangmulia	Cilacap Regional Hospital	± 1.5	11 – 13
Puri Tegalkamulyan Housing Complex	Wijaya Kusuma Stadium	± 1.8	14 – 16
Griya Tegal Asri Housing Complex	Al Jihad Mosque	± 2.6	19 – 23
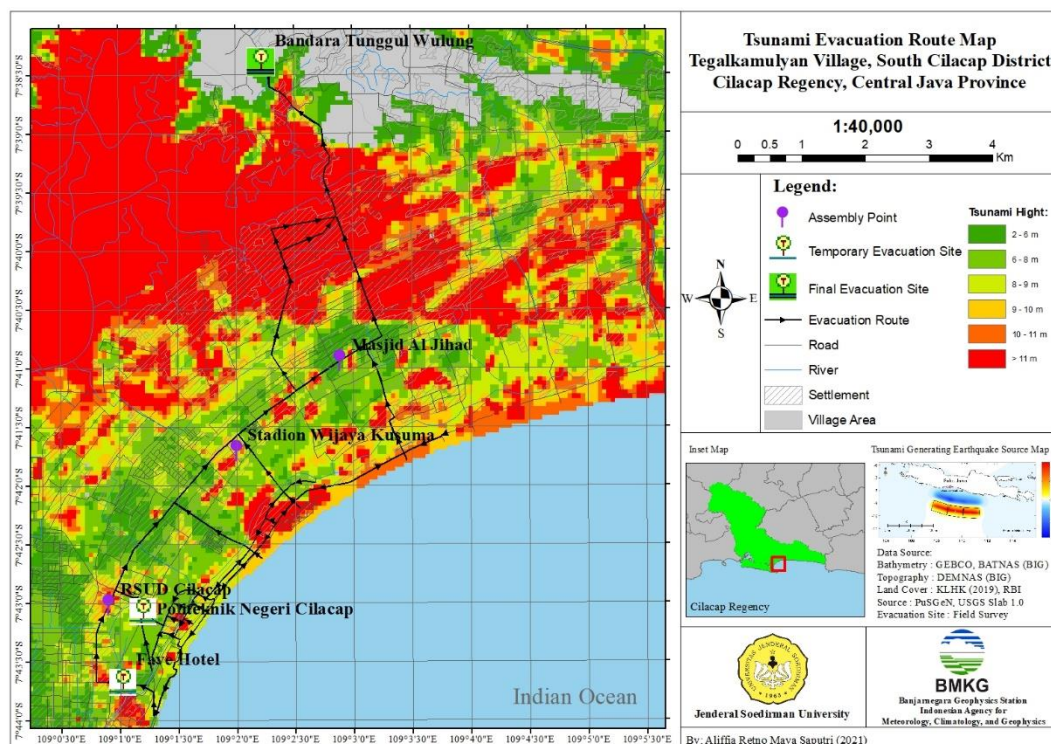
Figure 13. Tsunami evacuation route map for worst case scenario.

4. Conclusion

The tsunami source design can be described through the initial conditions of the tsunami, which produces vertical displacement with a wave increase of 11,418 m and a wave decrease of -7,476 m, where tsunami waves propagated from the earthquake source in all directions, with the fastest wave arrival time being 44 minutes and 1 second after the earthquake. Based on wave height, almost the entire Tegalkamulyan area is categorized as very dangerous, with several regions rated as hazardous. Worst-case scenario 5 modeling results show maximum flooding up to 12,700 km from the coastline, covering an area of 534,890 km² and reaching a maximum tidal wave height of 30,847 m. Based on the tsunami evacuation route map, vertical evacuation efforts direct people to immediately look for tall buildings and move towards the TES with an estimated time of approximately 6 – 23 minutes on foot, while horizontal evacuation efforts direct people in the TES to head towards the TEA with an estimated time of approximately 13 – 20 minutes at an average speed of 38 km/hour using motorized vehicles.

Acknowledgement

References

[1] GTZ, "Technical Documentation of Tsunami Hazard Map for Cilacap Regency," Cilacap: Cilacap Working Group for Tsunami Hazard Mapping, 2010.

[2] L.U. Khasanah, Suwarsito, and E. Sarjanti, "Level of Tsunami Disaster Vulnerability in the South Coast Area of Cilacap Regency," Geoeducation, vol. 3, no. 2, pp. 77-82, 2014.

[3] D. Mardiatno, MN Malawani, and RM Nisaa, "The future tsunami risk potential as a consequence of building development in Pangandaran Region, West Java, Indonesia," International Journal of Disaster Risk Reduction, vol. 46, no. 101523, 2020.

[4] S. Widiyantoro, E. Gunawan, A. Muhari, N. Rawlinson, J. Mori, NR Hanifa, S. Susilo, P. Supendi, HA Shiddiqi, AD Nugraha, and HE Putra, "Implications for Megathrust Earthquakes and Tsunamis from Seismic Gaps South of Java, Indonesia," Scientific Reports, vol. 10, no. 1, pp. 1-11, 2020.

[5] W. Kurniawan, D. Daryono, IDK Kerta, and T. Triwinugroho, "Analysis of the Tsunami Early Warning System in the Sunda Strait Megathrust Zone to Achieve National Resilience," PENDIPA Journal of Science Education, vol. 6, no. 2, pp. 457-464, 2022.

[6] Banjarnegara Geophysical Station, "Tsunami Hazard Map of South Cilacap District, Cilacap Regency, Central Java Province," BMKG, 2021.

[7] MM Muqoddas, "The Effect of Manning Roughness on Inundation Modeling in Cilacap," Thesis, Tangerang: STMKG, 2018.

[8] NI Rahmawati, "Tsunami Modeling in the Banda Sea and Inundation Implications in the Affected Area,". Thesis, Surabaya: Sepuluh Nopember Institute of Technology, 2017.

[9] Hanks, T. C., & Kanamori, H. (1979). A moment magnitude scale. Journal of Geophysical Research: Solid Earth, 84(B5), 2348–2350.

[10] D. Wells and K. Coppersmith, "New Empirical Relationship among Magnitude, Rupture Length, Rupture Width, Rupture Area, and Surface Displacement," Bulletin of the Seismological Society of America, vol. 4, no. 84, pp. 974-1002, 1994.

[11] B. Papazachos, E. Scordilis, D. Panagiotopoulos, C. Papazachos, and G. Karakaisis, "Global Relations Between Seismic Fault Parameters and Moment Magnitude of Earthquakes," Bulletin of the Geological Society of Greece, vol. 36, no. 3, pp. 1482-1489, 2004.

[12] HT Bedahg, OH Rogi, and P. Hanny, "Analysis of Tsunami Disaster Vulnerability in Palu City," Spatial Journal, vol. 6, no. 2, pp. 432-439, 2019.

[13] K. Satake, "Earthquakes and Tsunamis," Tokyo: Earthquake Research Institute, University of Tokyo, 2012.

[14] IOC, "Tsunami Glossary," IOC Technical Series, p. 85, 2016.

[15] E. Susanto, I. Nurana, and AR Setyahagi, "Tsunami Run-up Modeling in the Coastal Area of West Sulawesi," GAW Bariri Bulletin (BGB), vol. 1, no. 2, pp. 87-93, 2020.

[16] H. Yanagisawa, "Numerical Simulation of Tsunami and its Application," Tohoku: Tohoku Gakuin University, 2011.

[17] K. Kajiura and N. Shuto, "Numerical Modeling of Free-Surface Flows That Are Two Dimensional in Plan," Tsunami in the Sea, no. 9, pp. 395-420, 1990.

[18] X. Wang, "User Manual For Comcot Version 1.7 (First Draft)," USA: Cornell University, 2009.

[19] Natsir, A. M, "Tsunami Disaster Mitigation Modeling at Losari Beach," Thesis. Surabaya: Sepuluh Nopember Institute of Technology, 2018.

[20] Kurniawan. T, & Laili. A. F, "Determination of the Area Affected by the 'Maximum Tsunami Height' on the Island of Bali Based

Tsunami Evacuating Route Mapping..Aliffia Retno Maya Saputri, et. al

143

on the Potential for Tsunami-Generating Earthquakes in the Sumba Megathrust Segment," Journal of Disaster Management Dialogue, vol. 10, no. 1, pp. 93-104, 2019.

[21] Syukri A. and Mukhlis, "Study of Horizontal Tsunami Evacuation Routes in Padang Pariaman Regency," Civil Engineering, vol. 13, no. 2, pp. 1-12, 2016.

[22] National Earthquake Study Center Team, "2017 Map of Earthquake Sources and Hazards in Indonesia," Bandung: Center for Housing and Settlement Research and Development, 2017.

[23] GEBCO Compilation Group. (2021). GEBCO 2021 Grid.

[24] Geospatial Information Agency (BIG). (2018). National Digital Elevation Model (DEMNAS). Cibinong: Geospatial Information Agency (BIG).

[25] Muqoddas, A. (2018). Analysis of the Effect of Seafloor Roughness on Tsunami Simulation Using the COMCOT Model. Yogyakarta: Gadjah Mada University.

[26] S. Bilek and T. Lay, "Rigidity Variations with Depth Along Interplate Megathrust Faults in Subduction Zones," Nature, vol. 400, no. 6743, pp. 443-446, 1999.

[27] S. Khoiridah and BJ Santosa, "Estimation of Centroid Moment Tensor (CMT), Fault Plane, Rupture Duration, and Vertical Deformation Modeling of Earthquake Sources as a Study of Tsunami Hazard Potential in the South Java Sea," POMITS JOURNAL OF SCIENCE AND ARTS, vol. 3, no. 2, pp. 2337-3520, 2014.

[28] LW Aji, "Identification of Tsunami Evacuation Routes and Locations Based on FEMA P646 at Coastal Tourism Objects in Gunungkidul Regency (Case Study: Nguyahan, Ngobaran and Ngrenehan Beaches),"INERTIA, vol. 16, no. 1, pp. 24-37, 2020.

[29] Triatmadja and Radianta, "Tsunami Occurrence, Propagation, Destructive Power, and Mitigation," Yogyakarta: Gadjah Mada University Press, 2010.

[30] HH Latief, YP Sunendar, and E. Riawan, "Tsunami Inundation Modeling and Mapping and Tsunami Disaster Risk Assessment in Padang City," Bandung: PPKPL, ITB, 2006.